

**Figure 2.** Room temperature  $^{13}\text{C}$  spectra of free CO (185.5 ppm) in the presence of Pd colloid under 3 atm of  $^{13}\text{CO}$ . Each spectrum shows the region between 215 and 150 ppm, and the frequencies of the respective irradiation pulses are shown at the right. The PVP carbonyl peak at 178 ppm serves as internal reference. Each spectrum is the result of 600 acquisitions with a 1-s recycle delay, obtained by using a 10-mW 100-ms irradiation pulse.  $T_1$  for free CO was not measured, but changes in recycle delay near 1 s caused no variation in intensity. Inset: Plot of integrated intensity of the dissolved CO resonance vs irradiation frequency for "normal" (saturating) irradiation and "mirror image" (base line).

of 800 ppm (Figure 2), and a plot of the intensity of the free CO resonance vs irradiation frequency shows a broad minimum centered at 800 ppm. The shape of this saturation curve must of course depend not only on the line shape of the adsorbed CO resonance but also on the relative  $T_1$ 's and motional properties of CO molecules on the various sites in the sample (vide infra), but it is clear that the colloid-bound CO is strongly Knight shifted,<sup>4</sup> consistent with the presumed metallic nature of the colloid particles.

We tentatively ascribe the line width, which extends from 1200 to <300 ppm and is greater than that reported for CO on supported palladium at room temperature,<sup>5</sup> to a distribution of Knight shifts which vary with particle size (the colloid contains detectable numbers of particles ranging in size from 30 to 150 Å), and it would be expected that the smaller particles would be less shifted. Variation of pulse length and power produced little variation in the indirectly observed line shape. Clearly the observed line shape also is a function of the exchange rate between the dissolved CO and the adsorbed species and could also be affected by restricted surface diffusion of CO on the colloid particles caused by particle morphology and the presence of the PVP. Of course it is also possible that the width of the resonance reflects in part a slow, restricted tumbling of the colloid particles in the polymer solution. Approximate calculations can be made, using the Stokes-Einstein equation, of correlation times for motion of colloidal particles as a means of estimating the importance of motional effects on NMR line widths.<sup>7</sup> For particles of diameter 75 Å, correlation times of  $10^{-8}$  s are calculated, which would result in relatively narrow (<1 ppm) line widths, but the presence of PVP at the periphery of the palladium particles in our study would presumably result in some restriction of motion. Variable-temperature and "hole-burning" experiments<sup>8</sup> in a related colloidal palladium system<sup>1</sup> ruled out a significant contribution to the  $^{13}\text{C}$  line width of adsorbed CO from restricted motion in solution, and similar experiments are planned to investigate these possibilities in the present system. Interpretation of the indirectly observed line shape as a distribution of isotropic shifts of CO on the polydispersed colloid is consistent with the recent observation that magic angle spinning does not narrow the resonance of CO adsorbed on Pd/SiO<sub>2</sub>.<sup>5,9</sup>

(7) Yesinowski, J. P. *J. Am. Chem. Soc.* **1981**, *103*, 6266.

(8) (a) Duncan, T. M.; Thayer, A. M.; Root, T. W. *J. Chem. Phys.* **1990**, *92*, 2663. (b) Duncan, T. M.; Thayer, A. M.; Root, T. W. *Phys. Rev. Lett.* **1989**, *63*, 62.

The relative ease with which these experiments can be carried out with a colloidal metal sample presents the possibility that kinetic ligand exchange investigations can now be performed on the adsorption-desorption phenomena which play an important role in heterogeneous catalysis, using colloidal transition metals as an easily accessible analogue to supported catalyst particles. Colloid metals are active in numerous catalytic processes, and we anticipate NMR studies of working catalysts and of model colloid systems.

**Acknowledgment.** We thank S. B. Rice and K. Liang, of the Corporate Research Laboratory, Exxon Research and Engineering Company, for performing TEM and SAXS experiments, respectively, and a referee for drawing our attention to ref 7.

(9) Zilm, K. W.; Bonneviot, L.; Haller, G. L.; Han, O. H.; Kermarec, M. *J. Phys. Chem.* **1990**, *94*, 8495.

## Molecular Laminates. Three Distinct Crystal Packing Modes

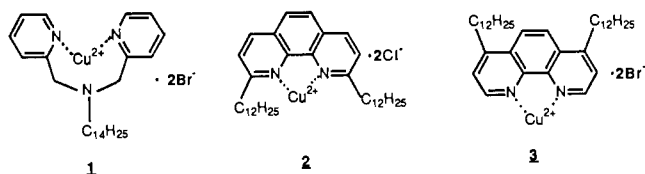
F. M. Menger,\* Jeng-Jong Lee, and K. S. Hagen

Department of Chemistry, Emory University  
Atlanta, Georgia 30322

Received January 30, 1991

Revised Manuscript Received March 18, 1991

Periodicity in crystalline solids leads to cooperative electronic effects and thus to materials with useful electrical, magnetic, and optical properties.<sup>1</sup> Yet the rational design of periodicity ("crystal engineering") remains a primitive art and an attractive area for further pursuit.<sup>2</sup> With this in mind (and with an ongoing affection for diverse organized assemblies of which crystals are the most perfect),<sup>3</sup> we set out to prepare crystalline solids with alternating layers of metal and hydrocarbon. Such "molecular laminates" were ultimately achieved via the three new long-chain copper complexes 1-3. As will be seen momentarily, the compounds crystallize into layered arrays, each with its own peculiar packing mode.



The ligand in 1 was synthesized from 2-picolyl chloride hydrochloride and 1-tetradecylamine in basic THF/water. The other two ligands were prepared by treatment of commercially available dimethylphenanthrolines with lithium diisopropylamide followed by 1-iodoundecane. Ligands were characterized by FAB-MS, NMR, and elemental analysis prior to their conversion into the copper chelates using CuCl<sub>2</sub> or CuBr<sub>2</sub> in absolute ethanol. X-ray quality crystals were obtained from methanol (1 and 2) and chloroform/acetonitrile (3).

Publications from England,<sup>4</sup> Germany,<sup>5</sup> Japan,<sup>6</sup> and Sweden<sup>7</sup> can be consulted for packing data on various long-chain compounds. Previous X-ray studies of layered compounds involving

(1) Mallouk, T. E.; Lee, H. *J. Chem. Educ.* **1990**, *67*, 829.

(2) Etter, M. C. *Acc. Chem. Res.* **1990**, *23*, 120. Desiraju, G. R. *Crystal Engineering: The Design of Organic Solids*; Elsevier: New York, 1989.

(3) Menger, F. M. *Angew. Chem.*, to be published.

(4) Hitchcock, P. B.; Mason, R.; Thomas, K. M.; Shipley, G. G. *Proc. Natl. Acad. Sci. U.S.A.* **1974**, *71*, 3036.

(5) Durfee, W. S.; Gruszecka, M.; Olszak, T. A.; Storck, W.; Bradaczek, H.; Willig, F. *J. Am. Chem. Soc.* **1989**, *111*, 3699.

(6) Okuyama, K.; Watanabe, H.; Shimomura, M.; Hirabayashi, K.; Kunitake, T.; Kajiyama, T.; Yasuoka, N. *Bull. Chem. Soc. Jpn.* **1986**, *59*, 3351. Okuyama, K.; Soboi, Y.; Hirabayashi, K.; Harada, A.; Kumano, A.; Kazuyama, T.; Takayanagi, M.; Kunitake, T. *Chem. Lett.* **1984**, 2117.

(7) Larsson, K. *Acta Crystallogr.* **1966**, *21*, 267. Pascher, I.; Sundell, S.; Hauser, H. *J. Mol. Biol.* **1981**, *153*, 807.

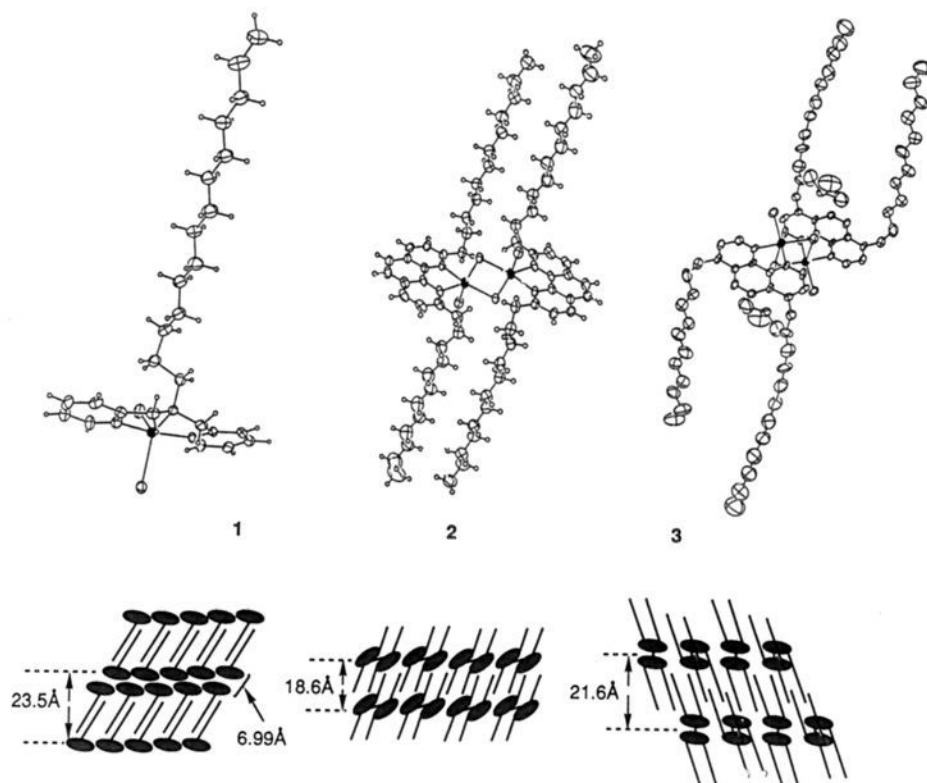


**Figure 1.** Molecular structures (30% thermal ellipsoids) and schematic packing diagrams for laminate compounds **1**, **2**, and **3**. Heavy dots in the former represent  $\text{Cu}^{2+}$ , and shaded circles in the latter represent  $\text{Cu}^{2+}$  plus the aromatic portion of the ligands. Hydrogens have been omitted from **3** for the sake of clarity.

heavy metals<sup>8,9</sup> are rare. Alternating polar and nonpolar layers along a crystallographic axis can occur in the absence of long chains.<sup>10</sup>

Figure 1 shows ORTEP representations of the copper complexes plus schematic drawings of their dispositions within the crystal lattices.<sup>11-13</sup> The main observations are now summarized: (a)

(8) Johnson, J. W.; Jacobson, A. J.; Butler, W. M.; Rosenthal, S. E.; Brody, J. F.; Lewandowski, J. T. *J. Am. Chem. Soc.* **1989**, *111*, 381.

(9) Day, P.; Ledsham, R. D. *Mol. Cryst. Liq. Cryst.* **1982**, *86*, 163.

(10) Lee, H.; Lynch, V. M.; Cao, G.; Mallouk, T. E. *Acta Crystallogr.* **1988**, *C44*, 365.

(11) Compound **1**: green crystals, triclinic space group  $P\bar{1}$ , with  $a = 7.516$  (7) Å,  $b = 8.455$  (7) Å,  $c = 23.822$  (18) Å,  $\alpha = 80.74$  (6)°,  $\beta = 87.43$  (7)°,  $\gamma = 69.30$  (6)°,  $V = 1397$  (2) Å<sup>3</sup>,  $d_{\text{calcd}} = 1.471$  g/cm<sup>3</sup>,  $d_{\text{obsd}} = 1.465$  g/cm<sup>3</sup>,  $Z = 2$ ,  $MW = 618.984$ , and  $\mu = 36.32$ . X-ray data were collected at 21 °C on a  $0.35 \times 0.3 \times 0.2$  mm crystal for 3113 independent reflections having  $3^\circ < 2\theta < 45^\circ$  on a Nicolet P3F four-circle diffractometer using graphite-monochromatized Mo K $\alpha$  radiation. The positions of the heavy atoms were solved via the Patterson method, and the remaining non-hydrogen atoms were found by difference Fourier syntheses, utilizing the SHELXTL program package. All non-hydrogen atoms were refined with anisotropic thermal parameters. The final residuals were  $R = 0.034$  ( $R_w = 0.039$ ) for 2452 data with  $I > 3\sigma(I)$ .

(12) Compound **2**: brown crystals, triclinic, space group  $P\bar{1}$ , with  $a = 9.629$  (3) Å,  $b = 10.200$  (4) Å,  $c = 19.065$  (9) Å,  $\alpha = 102.86$  (3)°,  $\beta = 89.93$  (3)°,  $\gamma = 101.06$  (3)°,  $V = 1790$  (1) Å<sup>3</sup>,  $d_{\text{calcd}} = 1.208$  g/cm<sup>3</sup>,  $d_{\text{obsd}} = 1.208$  g/cm<sup>3</sup>,  $Z = 1$ ,  $MW = 1302.61$ , and  $\mu = 7.51$ . X-ray data were collected at 21 °C on a  $0.15 \times 0.3 \times 0.4$  mm crystal for 4715 independent reflections having  $3^\circ < 2\theta < 45^\circ$  on a Nicolet P3F four-circle diffractometer using graphite-monochromatized Mo K $\alpha$  radiation. The structure was solved by direct methods utilizing the SHELXTL program package. All non-hydrogen atoms were refined with anisotropic thermal parameters. The final residuals were  $R = 0.048$  ( $R_w = 0.051$ ) for 3401 data with  $I > 3\sigma(I)$ .

(13) Compound **3**: black-brown crystals, monoclinic, space group  $P2_1/a$ , with  $a = 19.351$  (14) Å,  $b = 9.941$  (5) Å,  $c = 22.338$  (16) Å,  $\beta = 104.50$  (6)°,  $V = 4160$  (5) Å<sup>3</sup>,  $d_{\text{calcd}} = 1.37$  g/cm<sup>3</sup>,  $d_{\text{obsd}} = 1.35$  g/cm<sup>3</sup>,  $Z = 2$ ,  $MW = 1719.1674$ , and  $\mu = 24.48$ . X-ray data were collected at 21 °C on a  $0.2 \times 0.3 \times 0.4$  mm crystal for 3475 independent reflections having  $3^\circ < 2\theta < 40^\circ$  on a Nicolet P3F four-circle diffractometer using graphite-monochromatized Mo K $\alpha$  radiation. The positions of the heavy atoms were solved via the Patterson method, and the remaining non-hydrogen atoms were found by difference Fourier syntheses, utilizing the SHELXTL program package. All non-hydrogen atoms were refined with anisotropic thermal parameters. The final residuals were  $R = 0.048$  ( $R_w = 0.064$ ) for 2289 data with  $I > 3\sigma(I)$ .

All three compounds crystallize into molecular arrays where layers of hydrocarbon are interposed between layers of copper. (b) **1** packs with heavily interdigitated chains that are fully extended except for a single gauche linkage per chain. As indicated in the figure, the lattice is characterized by Cu-Cu distances of 6.99 and 23.5 Å. (c) **2** exists as a dimeric complex. Each aromatic ligand extends one of its chains upward and the other downward (again with a single gauche linkage per chain). The copper layers are only 18.6 Å apart. (d) **3** also exists as a dimeric complex, but (in contrast to **2**) both chains on a given aromatic ring project in the same direction. Only one of the two side-by-side chains contains a gauche linkage. An alternating arrangement within a particular copper layer is also evident. Copper layers are separated by 21.6 Å.

Dimeric complexes **2** and **3** possess four arms that extend from an aromatic core, and in this respect they resemble compounds known to form columnar mesophases.<sup>14</sup> However, experiments with a polarizing microscope (equipped with a variable-temperature stage) suggest that the compounds are nonmesogenic. A massive molecular reorganization would, of course, be required if the crystals were to interconvert with discotic states. Crystals that thermally transform into discotic mesophases are usually regarded as columnar themselves.

In summary, it is apparent that layer-to-layer distances in molecular laminates are affected by the number of chains, the length of the chains, and the location of the chains on the supporting scaffold. Information relating crystal packing to molecular structure will be critical to achieving a priori control of periodicity. At the moment, the goal is a distant one.

**Acknowledgment.** This work was supported by the National Institutes of Health.

(14) Gregg, B. A.; Fox, M. A.; Bard, A. J. *J. Chem. Soc., Chem. Commun.* **1987**, 1134. Ohta, K.; Hasebe, H.; Ema, H.; Fujimoto, T.; Yamamoto, I. *J. Chem. Soc., Chem. Commun.* **1989**, 1610. Sirlin, C.; Bosio, L.; Simon, J. J. *J. Chem. Soc., Chem. Commun.* **1988**, 236. Lehn, J.-M.; Malthête, J.; Levelut, A.-M. *J. Chem. Soc., Chem. Commun.* **1985**, 1794.

**Supplementary Material Available:** Details of the crystal structures of 1–3 including experimental procedures, ORTEP drawings, and tables of atomic positional parameters, bond distances, bond angles, anisotropic thermal parameters, hydrogen atom positions, and data collection parameters (33 pages); listing of observed and calculated structure factors for 1–3 (32 pages). Ordering information is given on any current masthead page.

## Cyclobutene Photochemistry.<sup>1</sup> Partial Orbital Symmetry Control in the Photochemical Ring Opening of a Constrained Cyclobutene

William J. Leigh\*<sup>2a</sup> and Kangcheng Zheng<sup>2b</sup>

Department of Chemistry, McMaster University  
Hamilton, Ontario, Canada L8S 4M1

Received February 11, 1991

Revised Manuscript Received March 22, 1991

Direct photolysis of alkyl-substituted cyclobutenes in solution results in competing, nonstereospecific ring opening to the corresponding conjugated dienes and fragmentation to the corresponding alkene and alkyne.<sup>3–8</sup> We have recently suggested that a nonconcerted mechanism best accounts for the results observed to date,<sup>5</sup> but there are alternative pericyclic pathways that cannot be completely ruled out. For example, if excited-state ring opening occurs entirely by the disrotatory route, then formally forbidden products could result if competing internal conversion to vibrationally excited levels of the cyclobutene ground state occurs or if excited-state ring opening proceeds adiabatically to yield diene(s) in the first excited singlet state.<sup>3,5</sup> Ring opening by the latter mechanism would be expected to yield a distribution of isomeric dienes that is determined by the excited-state torsional decay characteristics of the specific diene isomer(s) formed in the primary (disrotatory) step. In principle, this mechanism can be tested by comparing the diene distribution obtained from cyclobutene ring opening with that expected on the basis of the independently characterized excited-state behavior of the dienes, if the stable conformations of the dienes are similar to the (planar *s-cis*) conformers that would be initially obtained upon concerted ring opening.<sup>3,5</sup> With this goal in mind, we have initiated a study of the photochemistry of a series of polycyclic cyclobutene derivatives and their isomeric, conformationally constrained (*s-cis*) conjugated dienes. Our initial results, which are reported herein, reveal a fascinating structural dependence on the stereospecificity and efficiency of this prototypical excited-state pericyclic reaction.

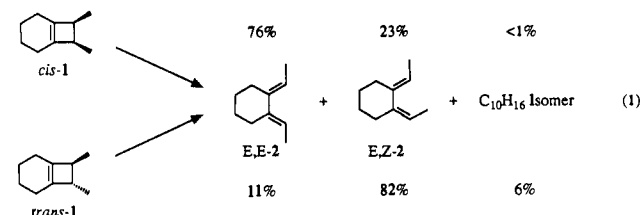
Direct photolysis of deoxygenated 0.02 M pentane solutions of *cis*- and *trans*-7,8-dimethylbicyclo[4.2.0]oct-1(6)-ene (**1**)<sup>9</sup> with

**Table I.** Product Quantum Yields from Photolysis (193 nm) of Deaerated 0.02 M Pentane Solutions of *cis*- and *trans*-**1** at 23 °C<sup>a</sup>

cyclobutene	( <i>E,E</i> )- <b>2</b>	( <i>E,Z</i> )- <b>2</b>	C <sub>10</sub> H <sub>16</sub> isomer
<i>cis</i> - <b>1</b>	0.57 ± 0.08	0.19 ± 0.03	
<i>trans</i> - <b>1</b>	0.09 ± 0.02	0.63 ± 0.09	0.05 ± 0.01

<sup>a</sup> Calculated from the slopes of concentration vs excitation dose plots, using the ring opening of bicyclo[4.2.0]oct-7-ene as actinometer.<sup>3</sup>

193- or 214-nm light<sup>11</sup> results in the formation of (*E,E*)- and (*E,Z*)-1,2-diethylidene-cyclohexane (**2**)<sup>12</sup> and one additional C<sub>10</sub>H<sub>16</sub> isomer in the yields shown in eq 1.<sup>13</sup> No other products were detected, in either case, in yields greater than 2% relative to that of the major product.<sup>14</sup> The relative product yields from photolysis of *cis*- and *trans*-**1** were independent of excitation wavelength in both cases.



Product quantum yields (Table I) were determined with the 193-nm light source. The photolysis of bicyclo[4.2.0]oct-7-ene, which yields *cis,cis*-1,3-cyclooctadiene with a quantum yield of  $0.14 \pm 0.02$ ,<sup>3</sup> was used as actinometer. The additional isomer formed on photolysis of *trans*-**2** could not be isolated owing to its low yield.

Quantum yields for *cis,trans* photoisomerization of (*E,E*)- and (*E,Z*)-**2** were determined by using a 254-nm light source and the direct photoisomerization of *cis,cis*-1,3-cyclooctadiene as actinometer ( $\phi_{cc \rightarrow ct} = 0.27$ ).<sup>15</sup> Under these conditions, direct photolysis of a deaerated 0.02 M pentane solution of (*E,E*)-**2** yields (*E,Z*)-**2** and *cis*-**1** with quantum yields of  $0.27 \pm 0.03$  and  $0.07 \pm 0.01$ , respectively. Photolysis of (*E,Z*)-**2** under identical conditions yields (*E,E*)-**2** and *trans*-**1** with quantum yields of  $0.28 \pm 0.03$  and  $0.025 \pm 0.005$ , respectively.<sup>16</sup> We note that ring closure of (*E,E*)- and (*E,Z*)-**2** occurs with >90% stereospecificity and with quantum yields similar to those reported for other *s-cis* dienes.<sup>17</sup> From the quantum yields for photoisomerization of **2**, the distributions of (*E,E*)- and (*E,Z*)-**2** that would be formed if ring opening of **1** occurs by the disrotatory adiabatic pathway can be calculated;<sup>18</sup> these are roughly (*E,E*)-**2**/*(E,Z)*-**2** = 2.4 and

(10) Owsley, D. C.; Bloomfield, J. J. *J. Org. Chem.* **1971**, *36*, 3768.

(11) Photolyses employed the pulses of an ArF excimer laser (193 nm, ca. 15 ns, 20 mJ, 0.5 Hz repetition rate) or a 16-W zinc resonance lamp (214 nm). Solutions were deoxygenated prior to photolysis with a stream of dry nitrogen.

(12) Compound (*E,E*)-**2** was prepared by semipreparative (ca. 300 mg) gas-phase thermolysis of *trans*-**1** at 180 °C. It was isolated by preparative vapor-phase chromatography after bulb-to-bulb distillation of the reaction mixture: <sup>1</sup>H NMR (CCl<sub>4</sub>)  $\delta$  1.58 (d, 6 H, *J* = 6.8 Hz), 1.59 (m, 4 H), 2.16 (br s, 4 H), 5.26 (q, 2 H, *J* = 6.8 Hz); UV (pentane)  $\lambda_{max}$  221 nm ( $\epsilon$  7500). Compound (*E,Z*)-**2** was isolated from the direct photolysis of (*E,E*)-**2** (see ref 9): <sup>1</sup>H NMR (CCl<sub>4</sub>)  $\delta$  1.60 (d, 3 H, *J* = 6.8 Hz), 1.60 (m, 4 H), 1.67 (d, 3 H, *J* = 6.8 Hz), 2.10 (m, 2 H), 2.74 (m, 2 H), 5.12 (complex m, 2 H); UV (pentane)  $\lambda_{max}$  216 nm ( $\epsilon$  8200). Complete spectroscopic data for these compounds will be reported in the full paper.

(13) Product yields were determined from the slopes of product concentration vs excitation dose plots, which were linear over the 0.5–4% conversion range. No other products were observed in yields greater than 3%. Control experiments in which 0.02 M solutions of **1** containing  $5 \times 10^{-4}$  M *cis,cis*-1,3-cyclooctadiene were photolyzed (193 and 214 nm) to ca. 5% conversion demonstrated that secondary diene photolysis does not occur under these conditions (no isomerization of the cyclooctadiene occurs).<sup>3,5,8</sup>

(14) The clean formation of only ring-opening products from **1** is noteworthy. In the other cases that have been studied, fragmentation competes effectively with ring opening;<sup>3–8</sup> in the case of **1**, however, this process would yield products of relatively high energy and is thus suppressed.

(15) Nebe, W. J.; Fonken, G. J. *J. Am. Chem. Soc.* **1969**, *91*, 1249.

(16) Photolysis of (*E,Z*)-**2** afforded one additional minor product, which was not identified, in ca. 0.010 quantum yield.

(17) (a) Srinivasan, R. *J. Am. Chem. Soc.* **1962**, *84*, 4141. (b) Chapman, O. L.; Pasto, D. J.; Borden, G. W.; Griswold, A. A. *J. Am. Chem. Soc.* **1962**, *84*, 1220. (c) Aue, D. H.; Reynolds, R. N. *J. Am. Chem. Soc.* **1973**, *95*, 2027. (d) Squillacote, M.; Semple, T. C. *J. Am. Chem. Soc.* **1990**, *112*, 5546.

(1) Part 7 of the series. Part 6: see ref 7.

(2) (a) Natural Sciences and Engineering Research Council of Canada University Research Fellow, 1983–1993. Author to whom correspondence should be addressed. (b) Permanent address: Department of Chemistry, Zhongshan University, Guangzhou, People's Republic of China.

(3) Clark, K. B.; Leigh, W. J. *J. Am. Chem. Soc.* **1987**, *109*, 6086.

(4) Leigh, W. J.; Zheng, K.; Clark, K. B. *Can. J. Chem.* **1990**, *68*, 1988.

(5) Leigh, W. J.; Zheng, K.; Clark, K. B. *J. Org. Chem.* **1991**, *56*, 1574.

(6) Dauben, W. G.; Haubrich, J. E. *J. Org. Chem.* **1988**, *53*, 600.

(7) Leigh, W. J.; Zheng, K.; Nguyen, N.; Werstiuk, N. H.; Ma, J. *J. Am. Chem. Soc.*, in press.

(8) Leigh, W. J.; Zheng, K. *J. Am. Chem. Soc.* **1991**, *113*, 2163.

(9) Compounds *cis*- and *trans*-**1** were synthesized as a 1:12 mixture by acetophenone-sensitized cycloaddition of 1,2,3,4-tetrahydrophthalic anhydride with 2-butene,<sup>10</sup> followed by hydrolysis and decarboxylation according to standard procedures.<sup>4,5</sup> The two isomers were separated and purified by semi preparative vapor-phase chromatography. Additional quantities of *cis*-**1** were prepared by direct photolysis (254 nm) of (*E,E*)-**2** (see ref 12). They were identified on the basis of their 500-MHz <sup>1</sup>H and <sup>13</sup>C NMR, IR, UV, and mass spectra. The <sup>1</sup>H NMR and UV spectra were particularly helpful in distinguishing between the two isomers.<sup>4</sup> *cis*-**1**: <sup>1</sup>H NMR (CCl<sub>4</sub>)  $\delta$  0.94 (d, 6 H, *J* = 6.7 Hz), 1.62 (m, 4 H), 1.75 (d, 2 H), 1.86 (d, 2 H), 2.78 (complex q, 2 H); UV (pentane)  $\lambda_{max}$  191 nm ( $\epsilon$  9400). *trans*-**1**: <sup>1</sup>H NMR (CCl<sub>4</sub>)  $\delta$  1.08 (d, 6 H, *J* = 6.8 Hz), 1.60 (m, 2 H), 1.66 (m, 2 H), 1.77 (d, 2 H, *J*  $\approx$  16 Hz), 1.85 (d, 2 H, *J*  $\approx$  16 Hz), 2.19 (complex q, 2 H, *J* = 6.5 Hz); UV (pentane)  $\lambda_{max}$  187 nm ( $\epsilon$  6300). Complete data will be reported in the full paper.